

Research Article

Padua points and “fake” nodes for polynomial approximation: old, new and open problems

STEFANO DE MARCHI*

ABSTRACT. Padua points, discovered in 2005 at the University of Padua, are the first set of points on the square $[-1, 1]^2$ that are explicitly known, unisolvent for total degree polynomial interpolation and with Lebesgue constant increasing like $\log^2(n)$ of the degree. One of the key features of the *Padua points* is that they lie on a particular *Lissajous curve*. Other important properties of Padua points are

- (1) in two dimensions, Padua points are a WAM for interpolation and for extracting approximate Fekete points and discrete Leja sequences.
- (2) in three dimensions, Padua points can be used for constructing tensor product WAMs on different compacts. Unfortunately, their extension to higher dimensions is still the biggest open problem.

The concept of mapped bases has been widely studied (cf. e.g. [35] and references therein), which turns out to be equivalent to map the interpolating nodes and then construct the approximant in the classical form without the need of resampling. The mapping technique is general, in the sense that works with any basis and can be applied to continuous, piecewise or discontinuous functions or even images. All the proposed methods show convergence to the interpolant provided that the function is resampled at the mapped nodes. In applications, this is often physically unfeasible. An effective method for interpolating via mapped bases in the multivariate setting, referred as *Fake Nodes Approach* (FNA), has been presented in [37]. In this paper, some interesting connection of the FNA with Padua points and “families of relatives nodes”, that can be used as “fake nodes” for multivariate approximation, are presented and we conclude with some open problems.

Keywords: Padua points, Lissajous curves and points, mapped polynomial basis.

2020 Mathematics Subject Classification: 41A17, 41A63.

1. INTRODUCTION

Let $\mathbb{P}_n(\mathbb{R})$ be the space of the univariate polynomials of total degree $\leq n$ on \mathbb{R} and $C(\mathbb{R})$ the linear space of continuous functions on \mathbb{R} . Further, for the basis of monomials $\mathcal{M} = \{1, x, x^2, \dots, x^n\}$ and a set $X = \{x_0, \dots, x_n\}$ of $n + 1$ distinct points, we denote by

$$(1.1) \quad Vdm(X; \mathcal{M}) = \prod_{i < j} (x_i - x_j)$$

the corresponding Vandermonde determinant which plays an important role for the unisolvency of a given set of points.

The classical univariate interpolation problem of f by polynomials of degree n can be stated as follows.

Problem 1. *Let K be a closed and bounded interval of \mathbb{R} . Consider X a set of $n + 1$ pairwise distinct points of K , the values $\{f(x_i), i = 0, \dots, n\}$ and the basis of monomials $\mathcal{M} = \{1, x, \dots, x^n\}$. Find the*

Received: 08.02.2022; Accepted: 01.03.2022; Published Online: 03.03.2022

*Corresponding author: Stefano De Marchi; stefano.demarchi@unipd.it

DOI: 10.33205/cma.1070020

polynomial $p_n = \sum_{k=0}^n a_k x^k$, so that

$$p_n(x_i) = f(x_i), \quad i = 0, \dots, n.$$

Being $x_i \neq x_j$, $i \neq j$, p_n is unique because $Vdm(X; \mathcal{M}) \neq 0$. Using the *Lagrange basis* $L = \{l_i, i = 0, \dots, n\}$ with

$$l_i(x) = \prod_{i=0, i \neq j}^n \frac{x - x_j}{x_i - x_j} = \frac{Vdm(X_i; \mathcal{M})}{Vdm(X; \mathcal{M})},$$

where X_i is the set X in which we substitute x_j with x , we can then write

$$(1.2) \quad p_n(x) = \sum_{i=0}^n l_i(x) f(x_i), \quad x \in K.$$

This process generates an interpolation error $e_n(x) = |f(x) - p_n(x)|$, $x \in K$ or in norm $E_n = \|f - p_n\|_\infty$. Using the Lagrange form (1.2) of the interpolant, we can bound this error by

$$(1.3) \quad E_n \leq (1 + \Lambda_n) E_n^*$$

with $\Lambda_n = \sup_{x \in K} \sum_{i=0}^n |l_i(x)|$ the *Lebesgue constant* which depends on n and on the node set X . As well-known, Λ_n represents the sup-norm of the linear operator (cf. e.g. [26]) $L : C(\mathbb{R}) \rightarrow \mathbb{P}_n(\mathbb{R})$, $Lf = \sum_{i=0}^n f(x_i) l_i$, where E_n^* is the error of best-uniform approximation that is $E_n^* := \inf_{p_n \in \mathbb{P}_n(\mathbb{R})} E_n(f)$.

In the one dimensional case we know

- $\Lambda_n \approx 2^n$ when the set X is made of equally spaced points of K (or even worse when X are randomly chosen);
- $\Lambda_n \approx \log(n)$ when X is made of *Chebyshev-like* points of K .

We call *Chebyshev-like* points, those points that have the so-called *arccos-distribution* which characterizes for instance the Chebyshev-Gauss-Lobatto points (or Chebyshev extrema)

$$\left\{ x_k = -\cos\left(\frac{k\pi}{n}\right), k = 0, \dots, n \right\}$$

and all zeros of orthogonal polynomials on a finite interval with respect to some positive measure. All these points are *near-optimal* in the sense that their Lebesgue constant grows logarithmically with respect to the degree n . Two other important sets of points are *Fekete points* and *Leja sequences* (cf. e.g. [32]) whose definition and properties will be discussed later on in the paper.

Fundamental question: Are there quasi-optimal interpolation nodes explicitly known in the multivariate setting for polynomial interpolation of total degree?

The answer is partially negative, *except for some known cases and in small dimensions* (see also the seminal paper by L. Bos [5]).

The previous question was the spring which pushed us in studying new families of near-optimal points, starting from the square $[-1, 1]^2$, being the square a simple domain, intrinsically tensorial, easy to be mapped to other domains (see [23]).

There are then many other questions and many more open problems, in this paper we present the answers to the following that were the main reasons why we discovered the *Padua points* on the square $\Omega = [-1, 1]^2$.

- We looked for *well-distributed nodes*. We found various nodal sets for polynomial interpolation of *even* degree n in the square Ω , which turned out to be equidistributed with respect to the *Dubiner metric* [45] and which show *near-optimal Lebesgue* constant growth [20].

- We also required *efficient interpolant evaluation*: the interpolant should be constructed without solving the Vandermonde system whose complexity is $O(N^3)$, for each pointwise evaluation, with $N = \binom{n+2}{2}$ the dimension of the bivariate polynomials of total degree $\leq n$. Moreover, we looked for closed formulae.
- We required *efficient cubature formulas*: in particular a fast computation of cubature weights for non-tensorial cubature formulae.

The last two points were inspired by the *rule of 10* claimed by Nick L. Trefethen in [60] (also in a talk given in 2009 at the Dolomites Workshops in Alba di Canazei): a good implementation should last for 10 seconds, have a 10 digits precision and does not consist of more than 10 lines of executable code.

In section 2, we start by introducing the Dubiner metric and which is the one we used for the square. Then, in section 3 we recall the construction of the Padua points, their properties and outline some open problems. Section 4 is devoted to the description of the problem of approximating discontinuous functions, which was the main reason of studying the “fake” nodes. In Section 5, we then introduce the idea of the “fake” nodes approach and its equivalence with the mapping polynomial basis. Also in this section we outline some open problems and possible future developments. We finally conclude in Section 6.

As a final note, many of the figures are taken from the papers cited in the bibliography of which I am a co-author and that can be reproduced with the Matlab codes freely available online.

2. FROM DUBINER METRIC TO PADUA POINTS

In his seminal paper [45], M. Dubiner introduced what we call the *Dubiner metric* which in $[-1, 1]$ corresponds to the arccosine distance between two points:

$$(2.4) \quad \mu_{[-1,1]}(x, y) = |\arccos(x) - \arccos(y)|, \quad \forall x, y \in [-1, 1].$$

By using the *Van der Corput-Schaake inequality* for trigonometric polynomials $T(\theta)$ of degree m and $|T(\theta)| \leq 1$, that is,

$$(2.5) \quad |T'(\theta)| \leq m \sqrt{1 - T^2(\theta)}$$

we want to show that the Dubiner metric is

$$(2.6) \quad \mu_{[-1,1]}(x, y) := \sup_{\|P\|_{\infty,[-1,1]} \leq 1} \frac{1}{m} |\arccos(P(x)) - \arccos(P(y))|$$

with $P \in \mathbb{P}_m([-1, 1])$. Firstly, inequality (2.5) is equivalent to

$$(2.7) \quad \left| \frac{d}{d\theta} \arccos(T(\theta)) \right| \leq m.$$

The following result then holds.

Lemma 2.1. *Take $x, y \in [-1, 1]$ and $P \in \mathbb{P}_m([-1, 1])$, then*

$$|\arccos(x) - \arccos(y)| = \sup_{\|P\|_{\infty,[-1,1]} \leq 1} \frac{1}{m} |\arccos(P(x)) - \arccos(P(y))|.$$

Proof. Letting $T(\theta) = P(\cos(\theta))$ and $x = \cos(\theta_x)$, $y = \cos(\theta_y)$. By using (2.7), we get

$$|\arccos(T(\theta_x)) - \arccos(T(\theta_y))| = \int_{\theta_x}^{\theta_y} \left| \frac{d}{d\theta} \arccos(T(\theta)) \right| d\theta \leq \int_{\theta_x}^{\theta_y} m d\theta \leq m |\theta_x - \theta_y|.$$

But $\arccos(x) = \theta_x$, $\arccos(y) = \theta_y$ giving

$$|\arccos(T(\theta_x)) - \arccos(T(\theta_y))| \leq m |\arccos(x) - \arccos(y)|$$

and

$$\sup_{\|P\|_{\infty,[-1,1]} \leq 1} \frac{1}{m} |\arccos(P(x)) - \arccos(P(y))| = |\arccos(x) - \arccos(y)|.$$

This concludes the proof. □

This metric generalizes to compact sets $\Omega \subset \mathbb{R}^d$, $d > 1$ (see e.g. [32]):

$$\mu_{\Omega}(\mathbf{x}, \mathbf{y}) := \sup_{\|P\|_{\infty, \Omega} \leq 1} \frac{1}{m} |\arccos(P(\mathbf{x})) - \arccos(P(\mathbf{y}))|.$$

This metric is important because there is an interesting unproved conjecture quoted in [20]:

Conjecture 1. *Nearly optimal interpolation points on a compact $\Omega \subset \mathbb{R}^d$ are asymptotically equidistributed with respect to the Dubiner metric on Ω .*

Hence, once we know the Dubiner metric on a compact Ω , we have at least a method for producing “good” interpolation points.

For $d = 2$, let $\mathbf{x} = (x_1, x_2)$, $\mathbf{y} = (y_1, y_2)$

- Dubiner metric on the square, $S = [-1, 1]^2$:

$$(2.8) \quad \mu_S(\mathbf{x}, \mathbf{y}) = \max\{|\arccos(x_1) - \arccos(y_1)|, |\arccos(x_2) - \arccos(y_2)|\}.$$

- Dubiner metric on the disk, $D = \{\|\mathbf{x}\| \leq 1\}$:

$$(2.9) \quad \mu_D(\mathbf{x}, \mathbf{y}) = \left| \arccos \left(x_1 y_1 + x_2 y_2 + \sqrt{1 - x_1^2 - x_2^2} \sqrt{1 - y_1^2 - y_2^2} \right) \right|.$$

As an example, by using the previous definition of the Dubiner metric on the square, we can extract points from a discretization of the square itself. In Fig. 1, we show 496 Dubiner nodes (corresponding on taking $n = 30$), Random and Euclidean points as well as their Lebesgue constants. Notice that the

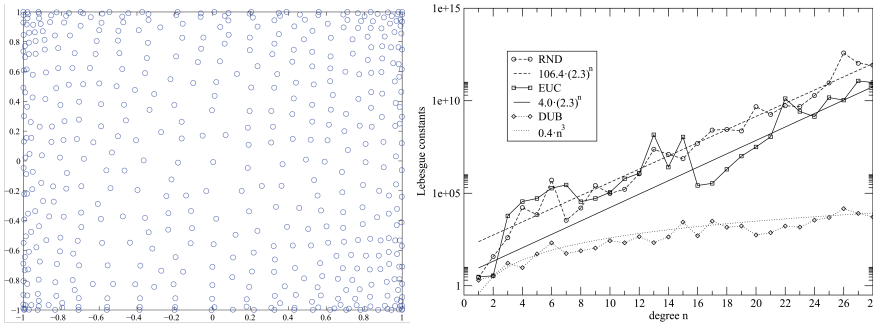


FIGURE 1. Left: Dubiner points. Right: Lebesgue constants growth.

Euclidean points, are *Leja-like* points, given by $\max_{\mathbf{x} \in \Omega} \min_{\mathbf{y} \in X_n} \|\mathbf{x} - \mathbf{y}\|_2$. There is a tight connection with the

Morrow-Patterson (MP)-points (see [63]) which are a set of $N = \binom{n+2}{2} = \dim(\mathbb{P}_n^2)$ points in the square $[-1, 1]^2$, equidistributed with respect to the Dubiner metric (2.8). To be more precise, let n be a positive even integer, the MP-points are given by the following

$$x_m = \cos\left(\frac{m\pi}{n+2}\right), \quad y_k = \begin{cases} \cos\left(\frac{2k\pi}{n+3}\right), & \text{if } m \text{ odd} \\ \cos\left(\frac{(2k-1)\pi}{n+3}\right), & \text{if } m \text{ even} \end{cases}$$

$1 \leq m \leq n + 1, 1 \leq k \leq n/2 + 1$ and are unisolvent for the total degree interpolation problem.

The interest of these points were noticed by Len Bos who showed, in an unpublished note, that their Lebesgue constant grows polynomially in n and $\Lambda_{MP} = O(n^6)$. Later on, in [39] we showed, by using (the reciprocal of) Christoffel functions for estimating the Lebesgue constant of the hyperinterpolation operator on various 2-dimensional domains, that indeed $\Lambda_{MP} = O(n^3)$. Numerically, we actually found a growth of $O(n^2)$. So this is an open problem to show that the $\Lambda_{MP} = O(n^2)$.

Brutman introduced the so-called *extended* Chebyshev points [17].

$$\tilde{T}_n = \left\{ \tilde{x}_k = -\frac{1}{\gamma_n} \cos\left(\frac{(2k-1)\pi}{2n}\right), k = 1, \dots, n \right\},$$

where $\gamma_n = \cos\left(\frac{\pi}{2n}\right)$, that is the set of Chebyshev points stretched to the boundary of the interval.

Similarly, we can define the *Extended Morrow-Patterson* points (EMP) as the points

$$x_m^{EMP} = \frac{1}{\alpha_n} x_m^{MP}, \quad y_k^{EMP} = \frac{1}{\beta_n} y_k^{MP},$$

$\alpha_n = \cos(\pi/(n+2)), \beta_n = \cos(\pi/(n+3))$.

Note: Both MP and the EMP points are equally distributed with respect to Dubiner metric on the square $[-1, 1]^2$ and unisolvent for polynomial interpolation of degree n on the square $[-1, 1]^2$ (see [20]). The *Padua points* (PD) are modified Morrow-Patterson points and were discovered “miraculously” in summer 2003, by Len Bos, Shayne Waldron, Marco Vianello and myself. They are the points in the square $[-1, 1]^2$ with coordinates

$$x_m^{PD} = \cos\left(\frac{(m-1)\pi}{n}\right), \quad y_k^{PD} = \begin{cases} \cos\left(\frac{(2k-1)\pi}{n+1}\right), & \text{if } m \text{ odd} \\ \cos\left(\frac{2(k-1)\pi}{n+1}\right), & \text{if } m \text{ even} \end{cases}$$

$$1 \leq m \leq n + 1, 1 \leq k \leq n/2 + 1, N = \binom{n+2}{2}.$$

We recall here some fundamental properties proved in [8].

- The PD points are equispaced with respect to Dubiner metric μ_S on $[-1, 1]^2$.
- The interior points are the MP points of degree $n - 2$ while the boundary points are “natural” points of the grid. In Fig. 2 to the left, we show the set of Padua points for $n = 8$ as well as the MP and EMP.
- There are 4 families of PD points obtained by taking rotations of 90 degrees: clockwise for *even* degrees and counterclockwise for *odd* degrees.
- The Lebesgue constant of the Padua points has optimal growth (see Fig. 2, right)

$$(2.10) \quad \Lambda(PD_n) = O((\log n)^2).$$

As a final note, their construction can be obtained in this simple way. Consider the $n + 1$ Chebyshev-Lobatto points on $[-1, 1]$

$$C_{n+1} = \left\{ z_j^n = \cos\left(\frac{(j-1)\pi}{n}\right), j = 1, \dots, n + 1 \right\}$$

and the two subsets of points with O=odd and E=even indexes

$$C_{n+1}^O = \left\{ z_j^n, j = 1, \dots, n + 1, j \text{ odd} \right\},$$

$$C_{n+1}^E = \left\{ z_j^n, j = 1, \dots, n + 1, j \text{ even} \right\}.$$

Then, the Padua points of degree n are the set

$$PD_n = C_{n+1}^O \times C_{n+2}^E \cup C_{n+1}^E \times C_{n+2}^O \subset C_{n+1} \times C_{n+2}.$$

As a nice and interesting observation, the Padua points lie on n concentric squares with sides at the zeros of U_n and U_{n-1} (the inner) except the external and the center [29]. With U_k we indicate the classical orthogonal Chebyshev polynomials of second kind, see also Fig. 3.

3. PADUA POINTS: GENERATING CURVE, WAMs, APPLICATIONS AND OPEN PROBLEMS

There exists an alternative construction consisting of the self-intersections and boundary contacts of the parametric and periodic curve, called *generating curve*:

$$\gamma(t) = \left(\underbrace{-\cos((n+1)t)}_{T_{n+1}(t)}, \underbrace{-\cos(nt)}_{T_n(t)} \right), \quad t \in [0, \pi].$$

For instance, in the figure below we display the curve $\gamma(t)$ for $n = 4$. The generating curve $\gamma(t)$ turns out to be a *Lissajous curve*. In particular, it is an algebraic curve such that $T_{n+1}(x) = T_n(y)$ (for the first family!). Being a Lissajous curve, we recall some important properties of these curves

- Their implicit equations can be found by using Chebyshev polynomials. Chebyshev polynomials are indeed Lissajous curves (cf. [62]).
- Lissajous curves are planar parametric curves studied by the astronomer Nathaniel Bowditch (1815) and later on by the mathematician Jules A. Lissajous (1857). They can be written in a general form as

$$\gamma(t) = (A_x \cos(\omega_x t + \alpha_x), A_y \sin(\omega_y t + \alpha_y)),$$

where A_x, A_y are amplitudes, ω_x, ω_y are pulsations and α_x, α_y are phases.

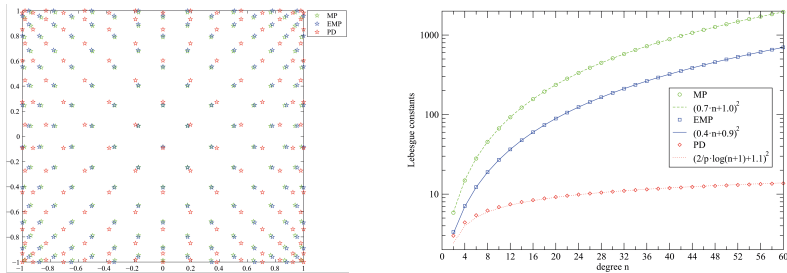


FIGURE 2. Left: the graphs of MP, EMP, PD for $n = 8$. Right: the growth of the corresponding Lebesgue constants.

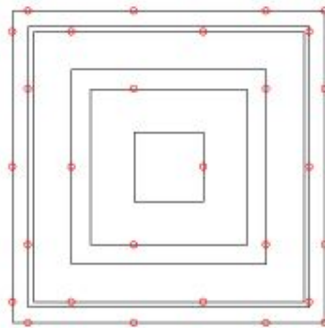


FIGURE 3. Padua for $n = 6$ are distributed on n concentric squares with sides at the zeros of U_n and U_{n-1} (the inner) except the external and the center (just a dot!).

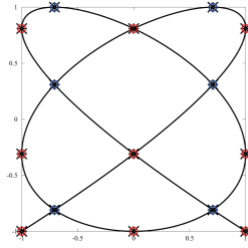


FIGURE 4. PD_4 on the generating curve and the two grids (with different colors).

In two dimensions, there is an interesting general definition described in [46].

Definition 3.1.

$$\gamma_{\kappa, \mathbf{u}}^n(t) = \begin{pmatrix} u_1 \cos(n_2 t - \kappa_1 \pi / (2n_1)) \\ u_2 \cos(n_1 t - \kappa_2 \pi / (2n_2)) \end{pmatrix}, \quad t \in [0, 2\pi],$$

with $\mathbf{n} = (n_1, n_2) \in \mathbb{N}^2$, $\boldsymbol{\kappa} = (\kappa_1, \kappa_2) \in \mathbb{R}^2$ and $\mathbf{u} = (u_1, u_2) \in \{-1, 1\}^2$. The values n_1, n_2 are called frequencies (like for the pendulum) and \mathbf{u} reflection parameter.

It is nice and also quite instructive to see how Lissajous curves can be constructed by playing with the *sand pendulum* (see the video <https://www.youtube.com/watch?v=7f16hAs1FB4>).

The construction in the square $[-1, 1]^2$ goes as follows. Let $\mathbf{n} = (n_1, n_2)$ with $n_1, n_2 \in \mathbb{N}$ relatively primes. Then, we may consider the curves $\gamma_\epsilon^n : [0, 2\pi] \rightarrow [-1, 1]^2$

$$(3.11) \quad \gamma_\epsilon^n(t) := \gamma_{(0, \epsilon-1), \mathbf{1}}^n(t) = \begin{pmatrix} \cos(n_2 t) \\ \cos(n_1 t + (\epsilon - 1)\pi / (2n_2)) \end{pmatrix}$$

with $\epsilon \in \{1, 2\}$ and fixed reflection parameter $\mathbf{1} = (1, 1)$.

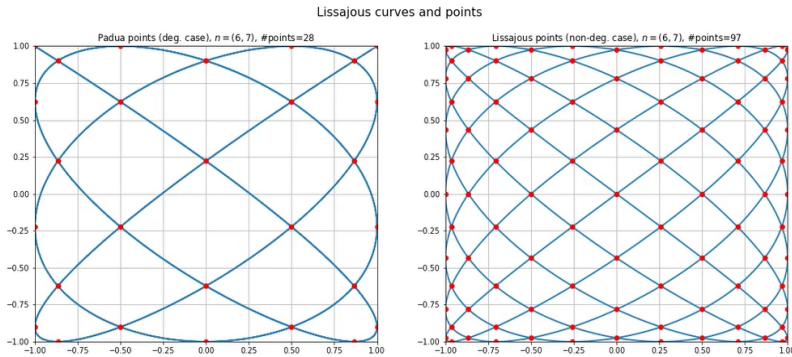


FIGURE 5. Left: Padua points, Right: Lissajous points. Both sets are relative to degree $\mathbf{n} = (6, 7)$, as used in (3.11).

Two special cases, whose details are discussed in [46], allow to classify Lissajous curves on the square in two main families.

- For $\epsilon = 1$, that is $\gamma_1^n(t)$, is called a *degenerate curve*.
- For $\epsilon = 2$, that is $\gamma_2^n(t)$, is called *non-degenerate curve*.

The Padua points curve is then a degenerate Lissajous curve, being two points of the curve at two consecutive corners of the square. Moreover, the degenerate Lissajous curve are π -periodic, while the non-degenerate are 2π periodic.

In Figure 5, we have displayed PD_6 and $Lis_{6,7}$. In particular the generating curves and the cardinalities are as follows:

$$\begin{aligned}\gamma_{n,n+1}^{PD} &= (\cos(nt), \cos((n+1)t)), \#PD_n = (n+2)(n+1)/2 \\ \gamma_{n_1,n_2}^{Lis} &= \left(\cos(n_2t), \cos(n_1t + \frac{\pi}{2n_2}) \right), \#Lis_{n_1,n_2} = 2n_1n_2 + n_1 + n_2.\end{aligned}$$

This shows that the Padua points are a unisolvent set for the total degree interpolation problem. While the Lissajous points can be used for polynomial interpolation, not of total degree, and they guarantee stability (slow growth of the Lebesgue constant).

The more general topic of multivariate polynomial approximation on Lissajous Curves turned out to be of interest in the emerging field of Magnetic Particle Imaging (MPI) (see, e.g., some recent publications and the activities of the scientific network MathMPI). Lissajous sampling seems to be relevant also in the field of Atomic Force Microscopy (AFM).

3.1. Padua points are WAM (Weakly Admissible Meshes). In the field of multivariate polynomial approximation, the notion of polynomial mesh has recently emerged as a significant concept. Originally introduced in the seminal paper [25], it has been studied in several subsequent papers, from both the theoretical and the computational point of view, interpolation and extracting Fekete points on 2d domains (cf. [14, 9, 12] and references therein). Moreover, approximate Fekete-like points extracted from polynomial meshes have begun to play a role in the framework of high-order methods for PDEs (cf., e.g., [83]).

We simply recall, that a polynomial *Weakly Admissible Mesh* (WAM) is a sequence of discrete subsets $\{A_n\}$ of a *polynomial determining* (i.e. polynomial vanishing there vanish everywhere) compact set $K \subset \mathbb{R}^d$ such that the inequality

$$(3.12) \quad \|p\|_K \leq C(A_n)\|p\|_{A_n}, \quad \forall p \in \mathbb{P}_n^d$$

holds, where both the $\text{card}(A_n) \geq \dim(\mathbb{P}_n^d) = \mathcal{O}(n^d)$ and $C(A_n)$ are bounded by n^d . Notice that $\|f\|_X$ is the sup-norm of a function f bounded on the (discrete or continuous) set X . Properties of WAMs and various examples in one and two dimensional domains, are described in [41]. Hence, once we know a WAM, the computation of *discrete extremal sets*, can be done by numerical linear algebra techniques by using *greedy algorithms*. The interested reader can refer to [13, 12].

The following lemma is the fundamental result for the construction of WAMs by using tensor product strategies.

Lemma 3.2. *Let $p \in \mathbb{P}_n^1$ be a univariate algebraic polynomial, and C_n, \tilde{C}_n the Chebyshev and Chebyshev-Lobatto nodal sets, respectively. Let $t \in \mathbb{T}_n^1$ be a univariate trigonometric polynomial, and Θ_n the angular nodal set*

$$\Theta_n(\alpha, \beta) = \phi_\omega(\tilde{C}_{2n}) + \frac{\alpha + \beta}{2} \subset (\alpha, \beta), \quad \omega = \frac{\beta - \alpha}{2} \leq \pi,$$

where $\phi_\omega(r) = 2 \arcsin(\sin \frac{\omega}{2} r)$, $r \in [-1, 1]$. Then, the following polynomial inequalities hold

$$(3.13) \quad \|p\|_{[a,b]} \leq c_n \|p\|_{C_n}$$

$$(3.14) \quad \|p\|_{[a,b]} \leq c_n \|p\|_{\tilde{C}_n}$$

$$(3.15) \quad \|t\|_{[\alpha,\beta]} \leq c_{2n} \|t\|_{\Theta_n}$$

with $c_n = 1 + \frac{2}{\pi} \log(n+1)$.

Padua points can be used in 3-dimensional tensor product WAMs on different domains [43]. Knowing a WAM on a planar compact, say Ω , we can construct 3-dimensional WAMs for cones with base Ω and vertex y , which consists of all the segments connecting y with a point on Ω . Similarly the construction can be done for pyramids (which are cones with polygonal base) and truncated cones. The last is obtained by cutting the cone with a plane parallel to the base. We can also construct 3-dimensional WAMs for solid of rotation with cross section Ω and external axis r . The WAMs is then obtained by rotation of Ω by a given angle $\leq 2\pi$, around a coplanar line r .

For instance in Fig. 6, we show on the left the WAMs for a pyramid obtained by the tensor product of Padua points of degree 10 on the base and Chebyshev-Lobatto points along the z -axis, on the right the WAM on a portion of the torus with circular base. In both sets we have highlighted the approximate Fekete points extracted from the WAM by the greedy algorithm described in [13].

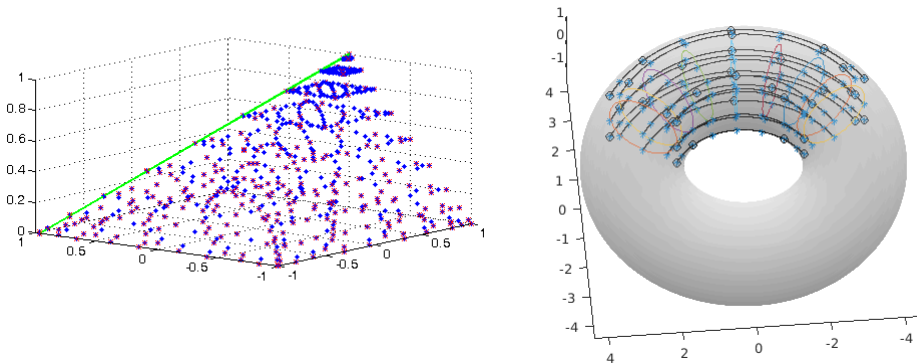


FIGURE 6. 3-dimensional WAMs obtained by using the Padua points.

3.2. Some recent applications of the Padua points. Lagrange interpolation at the Padua points has been recently used in several scientific and technological applications.

- Computational Chemistry (the Fun2D subroutine of the CP2K simulation package for Molecular Dynamics, <https://www.cp2k.org/>),
- Image Processing (algorithms for image retrieval by colour indexing),
- Materials Science (Modelling of Composite Layered Materials, [69]),
- Mathematical Statistics (Copula Density Estimation, [67]),
- Quantum Physics (Quantum State Tomography [59]),
- Padua points for solving PDEs with radial basis functions methods [58].

Padua points have been included in the *Chebfun2 package* (whose features have been described in the book [60]). The Padua points can be obtained simply specifying the degree n : `x=paduapts(n)`. For more details, see the web page <http://www.chebfun.org/examples/geom/Lissajous.html>

- **Software:** www.math.unipd.it/~marcov/CAApadua.html, J. Burkardt https://people.sc.fsu.edu/~jburkardt/m_src/padua/padua.html
- **Scholar citations (to the date): about 7140.**

3.3. Some open problems.

- (1) We do not know the Padua points on $[-1, 1]^d$, $d \geq 3$.

- (2) The Lebesgue function has its maxima in the corners, where there are no Padua points (see Fig. 7 that displays the Lebesgue function and its maximum at the corner points).
- (3) The Vandermonde determinant associated to the Padua and Padua-like points has variables that separate. Using a notation similar to (1.1), for a point set $A = \{a_1, \dots, a_N\} \in [-1, 1]^2$ and a basis $\mathcal{B} = \{b_1, \dots, b_N\}$, we may construct the Vandermonde matrix

$$V(A; \mathcal{B}) = (b_i(a_j))_{i,j=1}^N,$$

where the i -th row of V consists of i -th polynomial of the basis \mathcal{B} evaluated at all points. For Padua-like points $N = \binom{n+2}{2}$ and we denote with $Vdm(A; \mathcal{B})$ the corresponding determinant. Using the standard monomial basis of $\mathbb{P}_n(\mathbb{R}^2)$,

$$\mathcal{B}_n = \{x^\alpha y^\beta, | \alpha + \beta \leq n\},$$

the tensor product basis

$$\mathcal{T}_n = \{x^\alpha y^\beta, | \max(\alpha, \beta) \leq n\}$$

and the univariate polynomials

$$a(x) := \prod_{i=0}^{n/2} (x - x_{2i+1})$$

$$b(y) := \prod_{j=0}^{n/2} (y - y_{2j+1}),$$

another basis for $\mathbb{P}_n(\mathbb{R}^2)$ is

$$(3.16) \quad \mathcal{B}' = a(x)\mathcal{B}_{n/2-1} \cup b(y)\mathcal{B}_{n/2-1} \cup \mathcal{T}_n$$

such that $Vdm(A; \mathcal{B}_n) = \pm Vdm(A; \mathcal{B}'_n)$ being the transition matrix diagonal with 1 on the diagonal. This construction allowed to manipulate the Vandermonde matrix splitting it along the even and odd grids of the Padua-like points, providing an unexpected commutative property of the Vandermonde determinant associated to each direction. The claim in [11, Lemma 1] had a "gap". After some years, the Lemma was completely proved [42]. Moreover, we noticed that this "commutative" property of the Vandermonde determinant associated to Padua-like points, holds for general functions and general rectangular grids [31].

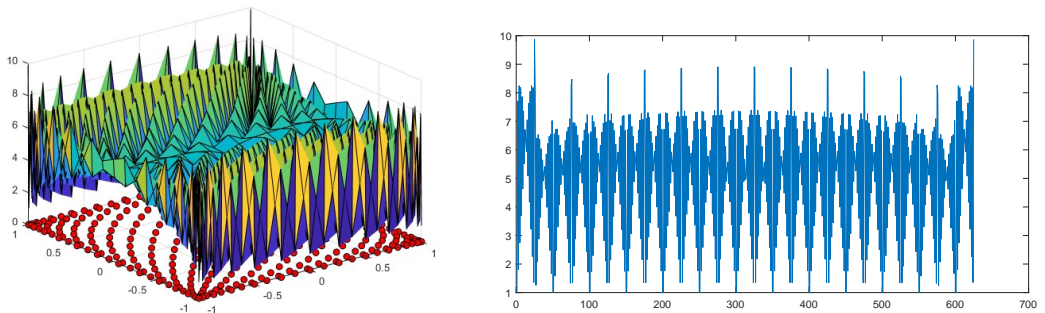


FIGURE 7. Padua points for $n = 25$ and its Lebesgue function. On the right the profile in 1d of the function.

4. APPROXIMATION OF DISCONTINUOUS FUNCTIONS

In this section, we deal with an important problem in data analysis, that is the reconstruction of functions with discontinuities or with jumps. The approach we describe is the *mapping bases technique* which turns out to be equivalent to the “fake” nodes approach [35, 37]. We recall that general approaches to overtake unavoidable reconstruction instabilities around the discontinuities are based on a clever choice of interpolation points before and after the jumps (cf. e.g. [33]), rational approximation (cf. e.g. [54, 4]), sinc-approx, filtering (cf. e.g. [36]). This list is not complete, but shows the wide interest to the topic. In particular, in image analysis in medicine (Computerized Tomography (CT), Magnetic Resonance (MR), and their variants (SPECT, fMRI)) or the above mentioned Magnetic Particle Imaging (MPI) or in geosciences, where satellite images are used to analyzed ground characteristics (humidity, temperature, water distribution and so on), often the images need to be geometrically aligned, registered or simply reconstructed by sampling them properly. In Figs. 8 and 9, we show some images connected to these applications.

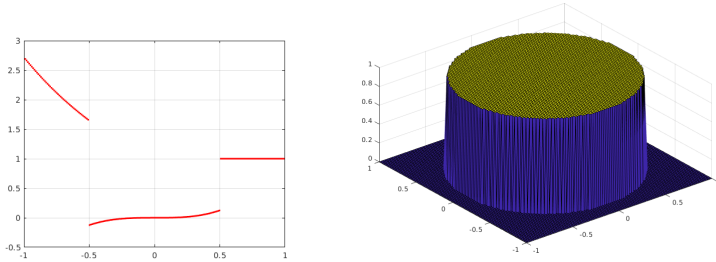


FIGURE 8. Discontinuous functions in 1d and 2d.

- Interpolation by polynomials and rational functions of discontinuous functions is historically well-studied. Two related well-known phenomena are the *Runge and Gibbs* effects [71, 51]. In both cases, unwanted oscillations appears near the boundary of the domain or close to the discontinuities, respectively.

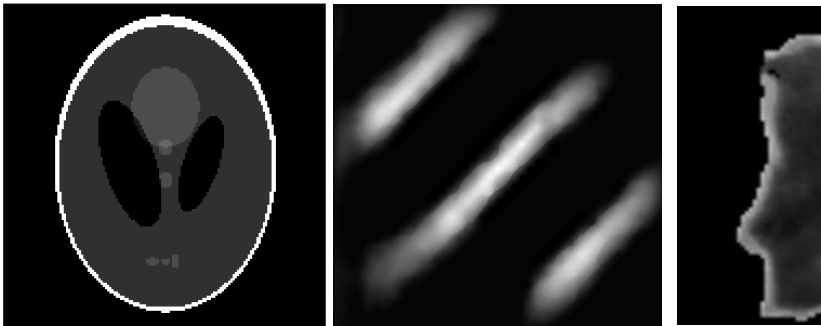


FIGURE 9. Left: the Shepp-Logan phantom used in medicine for testing. Center: an MPI acquisition reconstructed by Gaussian kernels. Right: RBF reconstruction of the soil of Portugal.

- More recently, interpolation by kernels, mainly radial basis functions has become a powerful tool for high-dimensional scattered data problems [52, 80, 18] and application to the solution of PDES [55], machine learning [72, 48], image registration and many other more.

5. THE FAKE NODES APPROACH (FNA)

We start observing three facts from which “fake” nodes ideas originated.

- (1) In applications, samples are given. *Resampling*, which is often necessary, can be done at Chebyshev points, or by extracting *mock Chebyshev* points from the data, or finding good interpolation points depending on applications (like Padua points, approximate Fekete points, discrete Leja sequences, Lissajous points, (P, f, β) -greedy points, minimal energy points and so on). For more details, see [35, 37].
- (2) When the function has steep gradients, like $f(x) = \arctan(20x)$, $x \in (-0.22, 0.22)$, its reconstruction gives rise to oscillations nearby the boundaries. This is a well-known fact from the Fourier analysis of the coefficients of the corresponding series known as *Gibbs phenomenon*.
- (3) For analytic functions on compact intervals, Adcock and Platte [1] investigated weighted least-squares approximation of mapped polynomial basis via the Kosloff and Tal-Azer map [57]:

$$\kappa_\alpha(x) = \frac{\sin(\alpha\pi x/2)}{\sin(\alpha\pi/2)}, \quad x \in [-1, 1], \quad \alpha \in (0, 1]$$

giving rise to the α -polynomial space

$$\mathbb{P}_n^\alpha = \{p \circ \kappa_\alpha, p \in \mathbb{P}_n\},$$

which corresponds to the space of trigonometric polynomials when $\alpha = 1$ and the classical polynomial space when $\alpha = 0$ (which is excluded).

These observations are the main ingredients of the FNA which, as we shall see, is equivalent to a polynomial mapping of the original polynomial space. We need some notations. Let $S : \Omega \rightarrow \mathbb{R}^d$ be an injective map. The main idea behind the FNA, is that of constructing an interpolant $R_f \in \mathcal{B}_N^S := \text{span}\{B_1^S, \dots, B_N^S\}$ of the function f , so that

$$(5.17) \quad R_f(\mathbf{x}) = \sum_{i=1}^N \alpha_i^S B_i^S(\mathbf{x}) = \sum_{i=1}^N \alpha_i^S B_i(S(\mathbf{x})) = P_g(S(\mathbf{x})), \quad \forall \mathbf{x} \in \Omega.$$

The function g has the property that $g|_{S(X_N)} = f|_{X_N}$, that is, it assumes the same values of f at the mapped interpolation points $S(X_N)$. Thus, having the mapped basis \mathcal{B}_N^S , the construction of the interpolant R_f is equivalent to build a classical interpolant $P_g \in \mathcal{B}_N$ at the “fake” or mapped nodes $S(X_N)$. In what follows we will use the words “*fake*” nodes, thinking of this mapping process.

Provided we have a unisolvent set of points for the given basis, $X_N = \{x_1, \dots, x_N\}$, and the corresponding values $\mathbf{f} = \{f(x_1), \dots, f(x_N)\}$, R_f can be constructed by solving the linear system

$$(5.18) \quad \mathbf{A}^S \boldsymbol{\alpha}^S = \mathbf{f},$$

where $\boldsymbol{\alpha}^S = (\alpha_1^S, \dots, \alpha_N^S)^\top$, and

$$\mathbf{A}^S = \begin{pmatrix} B_1^S(\mathbf{x}_1) & \dots & B_1^S(\mathbf{x}_N) \\ \vdots & \ddots & \vdots \\ B_N^S(\mathbf{x}_1) & \dots & B_N^S(\mathbf{x}_N) \end{pmatrix}.$$

Concerning the cardinal form of the mapped interpolant, we may state the following proposition.

Proposition 5.1 (Cardinal form). *Let $X_N = \{\mathbf{x}_i, i = 1, \dots, N\} \subseteq \Omega$ be a set of pairwise distinct data points and let $u_i \in \mathcal{B}_N, i = 1, \dots, N$ be the basis functions. Let $S : \Omega \rightarrow \mathbb{R}^d$ be an injective map. The functions $\{u_1, \dots, u_N\}$ are cardinal on $S(\Omega)$ for the “fake” nodes $S(X_N)$ if and only if the mapped functions $\{u_1 \circ S, \dots, u_N \circ S\}$ are cardinal for the original set of nodes X_N .*

The proof is trivial and comes immediately asking the cardinality property to the functions u_i^S . Hence, we can write the interpolant at the “fake” nodes in *cardinal* form:

$$(5.19) \quad R_f^S(\mathbf{x}) = \mathbf{f}^\top \mathbf{u}^S(\mathbf{x}), \quad \mathbf{x} \in \Omega,$$

where $\mathbf{u}^S(\mathbf{x}) = (u_1^S(\mathbf{x}), \dots, u_N^S(\mathbf{x}))^\top$.

The Lebesgue constant of the points mapped via R_f^S is equivalent to that of the image Ω though S (see [37] for details).

Proposition 5.2 (Equivalence of the Lebesgue constant). *Let $S : \Omega \rightarrow \mathbb{R}^d$ be an injective map. Let $X_N \subseteq \Omega$ be a unisolvent set of nodes for the space \mathcal{B}_N , and $u_i^S \in \mathcal{B}_N^S, i = 1, \dots, N$, be the associated cardinal functions. Then, the Lebesgue constant $\Lambda^S(\Omega)$ associated to the mapped nodes is*

$$\Lambda^S(\Omega) = \Lambda(S(\Omega)).$$

Remark 5.1. *The proposition states that the interpolation at the mapped basis \mathcal{B}_N^S inherits the Lebesgue constant of the “fake” nodes $S(X_N)$ over the ‘standard’ basis \mathcal{B}_N .*

The Lebesgue constant, as well-known, represents the stability constant of the interpolation process. For analyzing the stability, we thus study an interpolant of perturbed data $\tilde{f}(\mathbf{x}_i)$ sampled at $\mathbf{x}_i, i = 1, \dots, N$, i.e. data affected by measurement errors.

Proposition 5.3 (Stability). *Let $S : \Omega \rightarrow \mathbb{R}^d$ be an injective map and $X_N \subseteq \Omega$ be a unisolvent set of nodes for the space \mathcal{B}_N . Let \mathbf{f} be the associated vector of function values and $\tilde{\mathbf{f}}$ be the vector of perturbed values. Let R_f^S and $R_{\tilde{f}}^S$ be the interpolant of the function values \mathbf{f} and $\tilde{\mathbf{f}}$, respectively. Then,*

$$\|R_f^S - R_{\tilde{f}}^S\|_{\infty, \Omega} \leq \Lambda^S(\Omega) \|\mathbf{f} - \tilde{\mathbf{f}}\|_{\infty, X_N}.$$

Proof. Taking into account that $g|_{S(X_N)} = f|_{X_N}$ and thus also $\tilde{g}|_{S(X_N)} = \tilde{f}|_{X_N}$, we deduce that

$$\begin{aligned} \|R_f^S - R_{\tilde{f}}^S\|_{\infty, \Omega} &= \|P_g - P_{\tilde{g}}\|_{\infty, S(\Omega)} = \sup_{\mathbf{x} \in S(\Omega)} \left| \sum_{i=1}^N (g_i(\mathbf{x}_i) - \tilde{g}_i(\mathbf{x}_i)) u_i(\mathbf{x}) \right| \\ &= \sup_{\mathbf{x} \in \Omega} \left| \sum_{i=1}^N (g_i(S(\mathbf{x}_i)) - \tilde{g}_i(S(\mathbf{x}_i))) u_i(S(\mathbf{x})) \right| \\ &\leq \sup_{\mathbf{x} \in \Omega} \sum_{i=1}^N |u_i(S(\mathbf{x}))| |g_i(S(\mathbf{x}_i)) - \tilde{g}_i(S(\mathbf{x}_i))| \\ &\leq \sup_{\mathbf{x} \in \Omega} \sum_{i=1}^N |u_i(S(\mathbf{x}))| \max_{i=1, \dots, N} |g_i(S(\mathbf{x}_i)) - \tilde{g}_i(S(\mathbf{x}_i))| \\ &= \Lambda(S(\Omega)) \max_{i=1, \dots, N} |f(\mathbf{x}_i) - \tilde{f}_i(\mathbf{x}_i)| \\ &= \Lambda^S(\Omega) \|\mathbf{f} - \tilde{\mathbf{f}}\|_{\infty, X_N}. \end{aligned}$$

This concludes the proof. □

Consistently with Remark 5.1, the FNA approach also inherits the error of the classical approach, as shown in the following proposition.

Proposition 5.4 (Error bound inheritance). *Letting S , X_N , f and R_f^S , as above. Then, for any given function norm, we have*

$$\|R_f^S - f\|_\Omega = \|P_g - g\|_{S(\Omega)},$$

where $g|_{S(X_N)} = f|_{X_N}$.

Proof. From (5.17), we know that $R_f^S = P_g \circ S$. Choosing g such that $g \circ S = f$ on Ω (this g exists being S injective), we get

$$\|R_f^S - f\|_\Omega = \|P_g \circ S - g \circ S\|_\Omega = \|P_g - g\|_{S(\Omega)},$$

which gives the claimed result. \square

5.1. Mapped bases. As discussed above, let $S : I \rightarrow \mathbb{R}$ be a given map. We are interested to the function

$$(5.20) \quad R_{n,f}^S(x) := P_{n,g}(S(x)) = \sum_{i=0}^n c_i S_i(x)$$

for some $g : S(I) \rightarrow \mathbb{R} \in C^r(I)$ such that

$$g|_{S(X_n)} = f|_{X_n}.$$

$R_{n,f}^S \in \text{span}\{S_i = m_i \circ S, i = 0, \dots, n\}$ is the interpolant at (X_n, F_n) , that is no resampling is done. This mapping construction is equivalent to the “fake” nodes approach.

- The mapped bases approach on I ask to “interpolate f on the set X_n via $R_{n,f}^S$ in the function space S_n .”
- The FNA on $S(I)$ ask to “interpolate g on the set $S(X_n)$ via $P_{n,g}$ in the polynomial space M_n .”

Remark 5.2. *This approach is rather general, in the sense that we may use any space of linear independent functions (polynomials, rational function, radial basis functions and so on). The only point to clarify is the choice of the map S .*

Problem 2. *How can we find a suitable admissible map S for mitigating the Runge and Gibbs effects?*

The map S should be taken so that the resulting set of “fake” nodes $S(X_n)$ guarantees a stable interpolation process. A “natural” choice for a stable interpolation is to map X_n for example, to the set of Chebyshev-Lobatto (CL) nodes on the interval I .

The following algorithms, S -Runge and S -Gibbs, provide a constructive solution to Problem 2.

Algorithm 1 (S -Runge).

Input: X_n, C_n . *Note: X_n is ordered left-right, C_n are the CL nodes.*

Core

- If $x \in [x_i, x_{i+1}]$, for $i \in \{0, \dots, n-1\}$, S is the (piecewise) linear map

$$S(x) = \beta_{1,i}(x - x_i) + \beta_{2,i},$$

where

$$\beta_{1,i} = \frac{c_{i+1} - c_i}{x_{i+1} - x_i}, \quad \beta_{2,i} = c_i.$$

Output: $S(x)$.

For S -Gibbs, we need to identify the set of discontinuities

$$D_m := \{(\xi_i, d_i) \mid \xi_i \in (a, b), \xi_i < \xi_{i+1}, \text{ and } d_i := |f(\xi_i^+) - f(\xi_i^-)|\}, i = 0, \dots, m$$

by an edge-detection algorithm. This can be done by well-known and stable techniques, such as the the Canny algorithm described in [24] or, for irregularly samples signals and images, in [2]. When Radial basis functions are used, the analysis of the coefficients of the interpolant, can give information on the location of the discontinuities, as described in [70]. Recently, we proposed another approach to extract

the location of the discontinuities through a segmentation method based on a classification algorithm from machine learning (see [38]).

Algorithm 2 (S-Gibbs).

Inputs: X_n, D_m, x and $k \in \mathbb{R}_+$.

Core

(a) $\alpha_i := kd_i, i = 0, \dots, m$.

(b) Letting $A_i = \sum_{j=0}^i \alpha_j$, define S as follows:

$$S(x) = \begin{cases} x, & \text{for } x \in [a, \xi_0], \\ x + A_i, & \text{for } x \in [\xi_i, \xi_{i+1}[, 0 \leq i < m, \text{ or } x \in [\xi_m, b]. \end{cases}$$

Output: $S(x)$.

Remarks. Some comments are in order.

- Our strategy consists in constructing the map S in such a way that it sufficiently increases the gap between the node right before and the one right after the discontinuities via the real parameters α_i .
- About the shifting parameter $k > 0$. We experimentally observed that its selection is not critical. The resulting interpolation process is not sensitive to its choice, provided that it is sufficiently large, i.e. in such a way that in the mapped space the so-constructed function g has no steep gradients.
- The “fake” nodes mapping, S -Runge, enables one to obtain an interpolant on equispaced points that may converge efficiently while avoiding Runge phenomenon. The connection worth to be emphasized regards the application of this mapping on a polynomial basis. In particular, if we consider the Chebychev polynomials of the first kind, that is

$$T_k(x) = \cos(k \arccos(x)), \text{ for } x \in [-1; 1], k \geq 0,$$

then, it appears that applying the “fake” nodes mapping to T_k on a general interval $[a, b]$, provides a Fourier basis \hat{T}_k :

$$\hat{T}_k(x) = T_k(\cos(\pi(x - a)/(b - a))) = \cos(k\pi(x - a)/(b - a)).$$

In other words, interpolating with the “fake” nodes mapping is equivalent to a particular decomposition in Fourier series. It also means that one can make direct connections with several tricks used e.g. by the software `Chebfun` [64] and easily find the series coefficients via an FFT. An application of this idea has recently been explored in [56].

In Fig. 10, we plot the cardinal functions on 4 nodes (so cubics), at varying the location of the discontinuity ξ and the shift parameter k . The cardinals become discontinuous at ξ . When ξ is not at the center of the interval, they do not look anymore cubics.

5.2. Examples.

5.2.1. *Runge phenomenon.* The first example of the FNA deals with the interpolation of the *Runge function*. We take $I = [-5, 5]$, $f_1(x) = 1/(1 + x^2)$, X_n : equally spaced. As evaluation points we consider a set of 100 equally spaced points.

We computed the Relative Max Approximation Error (RMAE), that is

$$\text{RMAE} = \max_{z \in E} \frac{|R_{n,f}^s(z) - f(z)|}{|f(z)|},$$

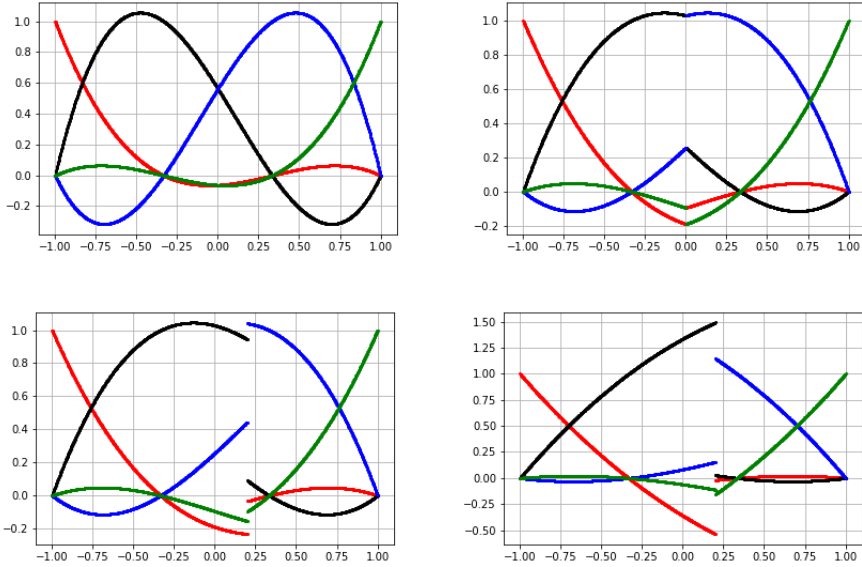


FIGURE 10. Left-right, up-down: the original cardinals on 4 nodes, the cardinals around $\xi = 0, k = 0$, the cardinals around $\xi = 0.2, k = 1$, the cardinals around $\xi = 0, k = 0.5$.

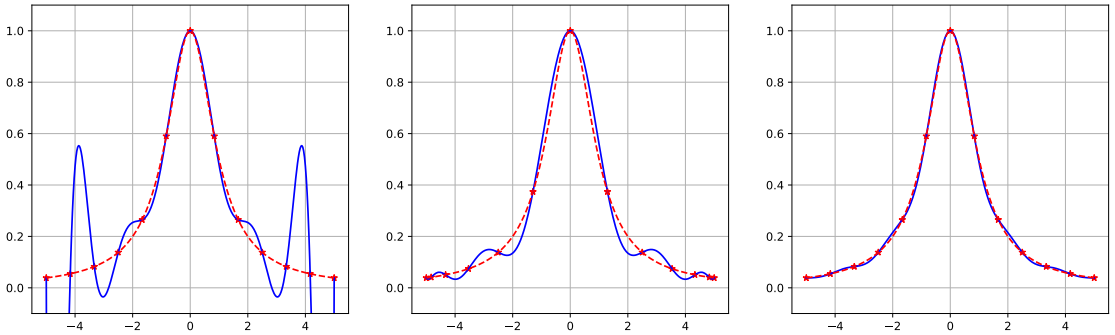


FIGURE 11. Interpolation at 13 points of f_1 . Using equispaced (left), CL (center) and “fake” nodes (right). The original and reconstructed functions are plotted with continuous red and dotted blue lines, respectively.

5.2.2. *Gibbs phenomenon.* The second example deals with the Gibbs effect. We consider the discontinuous function below

$$f_2(x) := \begin{cases} \frac{x^2}{10}, & -5 \leq x < -\frac{3}{2}, \\ \frac{1}{4}x + \frac{19}{8}, & -\frac{3}{2} \leq x < \frac{5}{2}, \\ -\frac{x^3}{30} + 4, & \frac{5}{2} \leq x \leq 5. \end{cases}$$

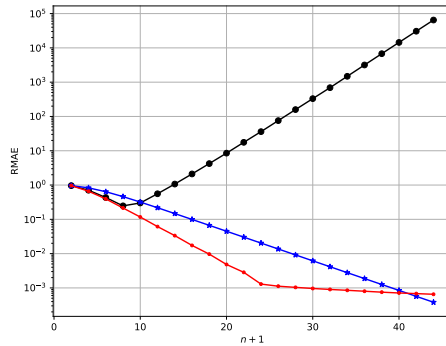


FIGURE 12. The RMAE for the Runge function varying the number of nodes. The results with equispaced, CL and “fake” nodes are represented by black circles, blue stars and red dots, respectively.

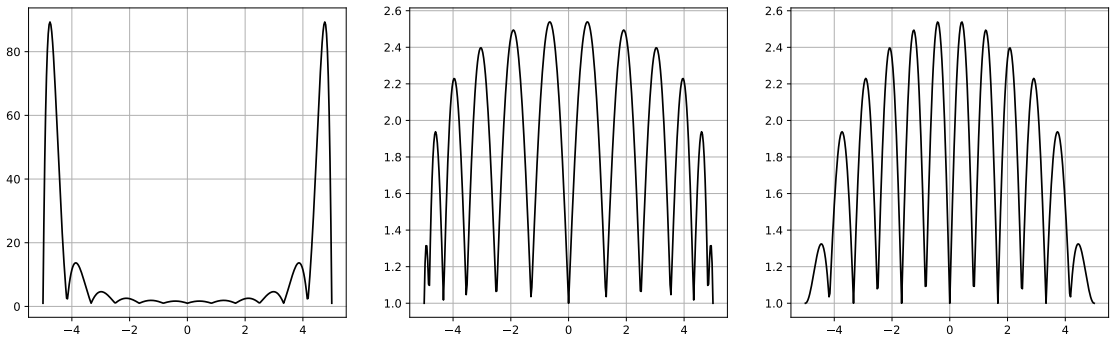


FIGURE 13. Lebesgue functions of equispaced (left), CL (center) and “fake” CL (right) nodes.

In this example $\mathcal{D} = \{(-3/2, 1.775), (5/2, 0.479)\}$. As before, we compare:

- the interpolating polynomial at equispaced points E_n and associated function values $f_2(E_n)$;
- the interpolating polynomial at the CL nodes C_n in I and resampled function values $f_2(C_n)$;
- the approximant built upon the polynomial interpolant at the “fake” nodes, $S(E_n)$, and function values related to the equispaced points $f_2(E_n)$. In this setting, we fix $k = 50$ and the map S of the S -Gibbs algorithm.

5.3. Extensions. The mapped basis approach suggested many interesting applications. Here, we enumerate the most interesting ones and the corresponding references in which interested readers can refer to.

- Quadrature weights of the “fake” Chebyshev-Lobatto nodes are those of the composite trapezoidal rule [34].
- In 2d and 3d, as we have already seen, we can extract approximate Fekete points on various domains (disk, sphere, polygons, spherical caps, lunes, etc.). With these points we can apply the mapped basis approach for least-squares approximation [37]. In the 2d case, we have results on the approximation of discontinuous functions on the square, using polynomial approximation at the Padua points or tensor product meshes, see Figs. 17 and 18. It is interesting to see Fig.

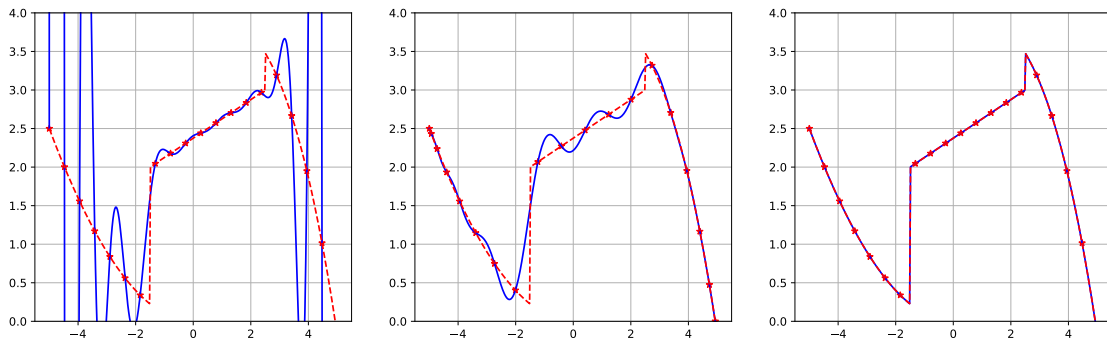


FIGURE 14. Interpolation at 20 points of the function f_2 on $[-5, 5]$, using equispaced (left), CL nodes (center) and the discontinuous map (right). The nodes are represented by stars, the original and reconstructed functions are plotted with continuous red and dotted blue lines, respectively.

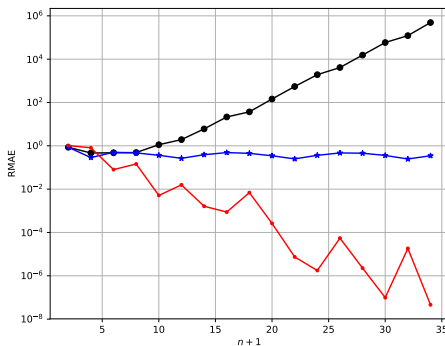


FIGURE 15. The RMAE for the function f_2 varying the number of nodes. The results with equispaced, CL and “fake” nodes are represented by black circles, blue stars and red dots respectively.

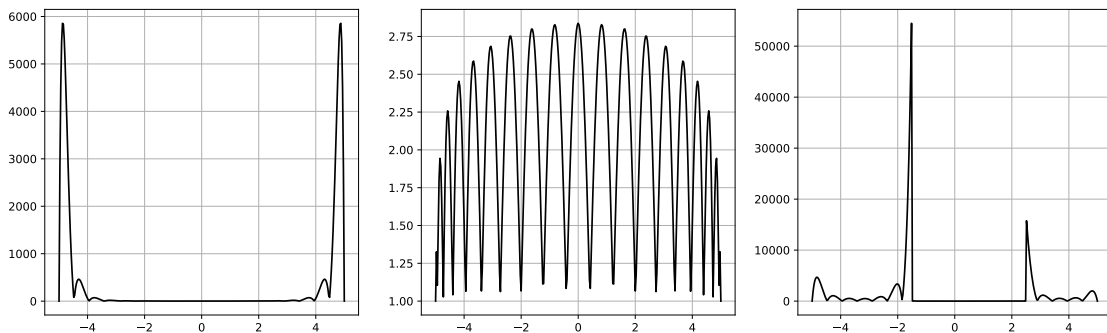


FIGURE 16. Lebesgue functions of equispaced (left), CL (center) and “fake” nodes (right).

18 where we show how to extract and map at the Padua points, *fake Padua*, starting from an original grid.

- In higher dimensions, where Padua points are not known, we may sample the function at the so-called Lissajous points or in the case of scattered data approximate by variably scaled discontinuous kernels [38].
- Extensions to rational interpolation/approximation: Floater-Hormann (FH) and trigonometric FH (for periodic signals) interpolants and the *AAA-approximation* (see [4] and references therein).
- The original proposed S-Gibbs map suffers of a subtle instability when the interpolation is done at equidistant nodes, a consequence of the Runge’s phenomenon. A new approach, termed *Gibbs-Runge-Avoiding Stable Polynomial Approximation (GRASPA)* has been introduced in [33], which allows to mitigate both Runge and Gibbs phenomena
- In multimodal medical imaging, it is a common practice to undersample the anatomically-derived segmentation images to measure the mean activity of a co-acquired functional image. This avoids the resampling-related Gibbs effect that would occur in oversampling the functional image. It turns out that the FNA for image resampling it is designed to reduce the Gibbs effect when oversampling the functional image. This has been proved by a tight error analysis in [66].
- Links: https://en.wikipedia.org/wiki/Runge%27s_phenomenon#S-Runge_algorithm_without_resampling

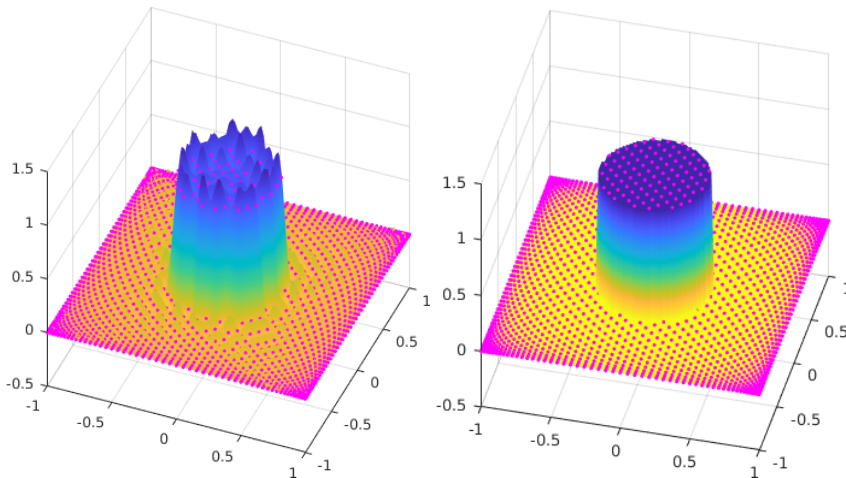


FIGURE 17. Left: interpolation with PD60 of a function with a circular jump. Right: the same by mapping circularly the PD points, and using least-squares fake-Padua.

5.4. Some open problems.

- As mentioned above, S-Runge and S-Gibbs have been improved in [33] via the GRASPA approach. Extension, at least to two dimensions, is needed.
- Recently two dimensional mock-Chebyshev points plus regression have been investigated [44]. Is this approach an alternative to the “fake” one?
- Error analysis and tight Lebesgue constant bounds should be investigated.

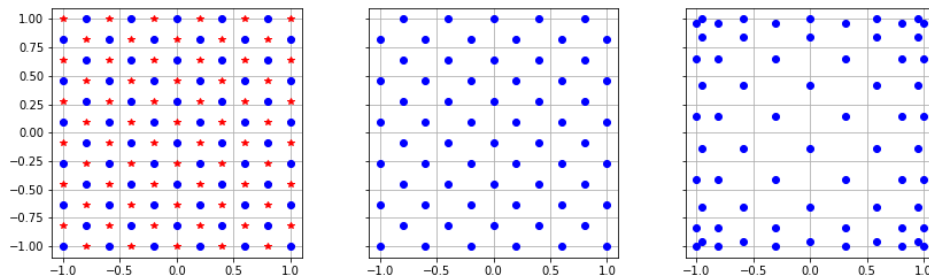


FIGURE 18. Here $n = 10$. On the left the set X_{66} (represented by blue dots) is extracted from a 11×12 equispaced grid (represented by both blue dots and red stars). The set X_{66} (centre) is then mapped on the set of Padua points Pad_{66} via the mapping S (right).

6. CONCLUSIONS

In this paper, we have reviewed the most important facts concerning the Padua points and the mapped bases approach for polynomial approximation of functions and data. We also outlined some open problems with the hope that some researcher can be interested in these topics and can propose a solution.

Acknowledgments. This work has been accomplished within the “Rete Italiana di Approssimazione” (RITA), the thematic group on “Approximation Theory and Applications” of the Unione Matematica Italiana (UMI). The paper in its final form, has been completed during the Erasmus mobility at the University “Lucian Blaga” of Sibiu, invited by Prof. A. Acu of the Department of Mathematics and Computer Science.

REFERENCES

- [1] B. Adcock, R. B. Platte: *A mapped polynomial method for high-accuracy approximations on arbitrary grids*, SIAM J. Numer. Anal., **54** (2016), 2256–2281.
- [2] R. Archibald, A. Gelb and J. Yoon: *Polynomial Fitting for Edge Detection in Irregularly Sampled Signals and Images*, SIAM J. Numer. Analysis, **43** (1) (2005), 259–279.
- [3] J. Baglama, D. Calvetti and L. Reichel: *Fast Leja points*, Electron. Trans. Numer. Anal., **7** (1998), 124–140.
- [4] J.-P. Berrut, S. De Marchi, G. Elefante and F. Marchetti: *Treating the Gibbs phenomenon in barycentric rational interpolation and approximation via the S-Gibbs algorithm*, Appl. Math. Letters, **103** (2020), 106196.
- [5] L. Bos: *On certain configurations of points in \mathbb{R}^n which are unisolvent for polynomial interpolation*, J. Approx. Theory, **64** (3) (1991), 271–280.
- [6] L. Bos: *Multivariate interpolation and polynomial inequalities*, Ph.D. course held at the University of Padua (2001), unpublished.
- [7] L. Bos, M. Caliari, S. De Marchi and M. Vianello: *A numerical study of the Xu interpolation formula*, Computing, **76** (3-4) (2006), 311–324.
- [8] L. Bos, M. Caliari, S. De Marchi, M. Vianello and Y. Xu: *Bivariate Lagrange interpolation at the Padua points: the generating curve approach*, J. Approx. Theory, **143** (1) (2006), 15–25.
- [9] L. Bos, J.-P. Calvi, N. Levenberg, A. Sommariva and M. Vianello: *Geometric Weakly Admissible Meshes, Discrete Least Squares Approximations and Approximate Fekete Points*, Math. Comp., **80** (2011), 1601–1621.
- [10] L. Bos, S. De Marchi, M. Vianello and Y. Xu: *Bivariate Lagrange interpolation at the Padua points: the ideal theory approach*, Numer. Math., **108** (1) (2007), 43–57.
- [11] L. Bos, S. De Marchi and S. Waldron: *On the Vandermonde Determinant of Padua-like Points (on Open Problems section)*, Dolomites Res. Notes on Approx., **2** (2009), 1–15.
- [12] L. Bos, S. De Marchi, A. Sommariva and M. Vianello: *Weakly Admissible Meshes and Discrete Extremal Sets*, Numer. Math. Theory Methods Appl., **4** (2011), 1–12.

- [13] L. Bos, S. De Marchi, A. Sommariva and M. Vianello: *Computing multivariate Fekete and Leja points by numerical linear algebra*, SIAM J. Num. Anal., **48** (5) (2010), 1984–1999.
- [14] L. Bos, N. Levenberg: *On the Approximate Calculation of Fekete Points: the Univariate Case*, Elec. Trans. Numer. Anal., **30** (2008), 377–397.
- [15] L. Bos, A. Sommariva and M. Vianello: *Least-squares polynomial approximation on weakly admissible meshes: disk and triangle*, J. Comput. Appl. Math., **235** (2010), 660–668.
- [16] L. Bos, M. A. Taylor and B. A. Wingate: *Tensor product Gauss-Lobatto points are Fekete points for the cube*, Math. Comp., **70** (2001), 1543–1547.
- [17] L. Brutman: *Lebesgue functions for polynomial interpolation: a survey*, Ann. Numer. Math., **4** (1997), 111–127.
- [18] M. D. Buhmann: *Radial Basis Functions: Theory and Implementation*, Cambridge Monogr. Appl. Comput. Math., Vol. 12, Cambridge Univ. Press, Cambridge, (2003).
- [19] CAA: Padova-Verona Research Group on Constructive Approximation webpage: <https://sites.google.com/view/caa-padova-verona/home>
- [20] M. Caliari, S. De Marchi and M. Vianello: *Bivariate polynomial interpolation on the square at new nodal sets*, Appl. Math. Comput., **165** (2) (2005), 261–274.
- [21] M. Caliari, S. De Marchi, M. Vianello: *Algorithm 886: Padua2D: Lagrange Interpolation at Padua Points on Bivariate Domains*, ACM Trans. Math. Software, **35** (3) (2008), 1–11.
- [22] M. Caliari, S. De Marchi and M. Vianello: *Bivariate Lagrange interpolation at the Padua points: computational aspects*, J. Comput. Appl. Math., **221** (2008), 284–292.
- [23] M. Caliari, S. De Marchi, A. Sommariva and M. Vianello: *Padua2DM: fast interpolation and cubature at Padua points in Matlab/Octave*, Numer. Algorithms, **56** (1) (2011), 45–60.
- [24] J. Canny: *A Computational Approach to Edge Detection*, IEEE Transactions on Pattern Analysis and Machine Intelligence, **8** (6) (1986), 679–698.
- [25] J. P. Calvi, N. Levenberg: *Uniform approximation by discrete least squares polynomials*, J. Approx. Theory, **152** (2008), 82–100.
- [26] W. Cheney, W. Light: *A Course on Approximation Theory*, AMS, Vol. 101, (2009).
- [27] K. C. Chung, T. H. Yao: *On lattices admitting unique Lagrange interpolations*, SIAM J. Numer. Anal., **14** (1977), 735–743.
- [28] P. Davis: *Interpolation and Approximation*, Blaisdell Pub Company, New York, (1963).
- [29] A. Cuyt, I. Yaman, B. A. Ibrahimoglu and B. Benouahmane: *Radial orthogonality and Lebesgue constants on the disk*, Numer. Algorithms, **61** (2) (2012), 291–313.
- [30] C. de Boor: *A Practical Guide to Splines*, revised edition, Springer, New York, (2001).
- [31] A. P. de Camargo, S. De Marchi: *A few remarks on "On certain Vandermonde determinants whose variables separate"*, Dolomites Res. Notes Approx., **8** (2015), 1–11.
- [32] S. De Marchi: *On Leja sequences: some results and applications*, Appl. Math. Comput., **152** (3) (2004), 621–647.
- [33] S. De Marchi, G. Elefante and F. Marchetti: *Stable discontinuous mapped bases: the Gibbs-Runge-Avoiding Stable Polynomial Approximation (GRASPA) method*, Comput. Appl. Math., **40**:299 (2021).
- [34] S. De Marchi, G. Elefante, E. Perracchione and D. Poggiali: *Quadrature at fake nodes*, Dolomites Res. Notes Approx., **14** Special Issue MATA2020 (2021), 39–45.
- [35] S. De Marchi, F. Marchetti, E. Perracchione and D. Poggiali: *Polynomial interpolation via mapped bases without resampling*, J. Comput. Appl. Math., **364** (2020), 112347.
- [36] S. De Marchi, W. Erb and F. Marchetti: *Lissajous sampling and spectral filtering in MPI applications: the reconstruction algorithm for reducing the Gibbs phenomenon*, 2017 International Conference on Sampling Theory and Applications SampTA (2017), 580–584.
- [37] S. De Marchi, F. Marchetti, E. Perracchione and D. Poggiali: *Multivariate approximation at fake nodes*, Appl. Math. Comput., **391** (2021), 125628.
- [38] S. De Marchi, W. Erb, F. Marchetti, E. Perracchione and M. Rossini: *Shape-Driven Interpolation with Discontinuous Kernels: Error Analysis, Edge Extraction and Applications in Magnetic Particle Imaging*, SIAM J. Sci. Comput., **42** (2) (2020), B472–B491.
- [39] S. De Marchi, A. Sommariva and M. Vianello: *Multivariate Christoffel functions and hyperinterpolation*, Dolomites Res. Notes Approx., **7** (2014), 36–33.
- [40] S. De Marchi, R. Schaback and H. Wendland: *Near-Optimal Data-Independent Point Locations for Radial Basis Function Interpolation*, Adv. Comput. Math., **23** (3) (2005), 317–330.
- [41] S. De Marchi, F. Piazzon, A. Sommariva and M. Vianello: *Polynomial Meshes: Computation and Approximation*, Proceedings of the 15th International Conference on Computational and Mathematical Methods in Science and Engineering CMMSE (2015), 414–425.
- [42] S. De Marchi, K. Usevich: *On certain multivariate Vandermonde determinants whose variables separate*, Linear Alg. Appl., **449** (2014), 17–27.

- [43] S. De Marchi, M. Vianello: *Polynomial approximation on pyramids, cones and solids of rotation*, Dolomites Res. Notes Approx., Proceedings DWCAA12, **6** (2013), 20–26.
- [44] F. Dell’Accio, F. Di Tommaso and F. Nudo: *Generalizations of the constrained mock-Chebyshev least squares in two variables: Tensor product vs total degree polynomial interpolation*, Appl. Math. Letters, **125** (2022), 107732.
- [45] M. Dubiner: *The theory of multi-dimensional polynomial approximation*, J. Anal. Math., **67** (1995), 39–116.
- [46] W. Erb, C. Kathner, P. Denker and M. Alhborg: *A survey on bivariate Lagrange interpolation on Lissajous nodes*, Dolomites Res. Notes Approx., **8** (2015), 23–36.
- [47] G. E. Fasshauer: *Meshfree Approximation Methods with Matlab*, World Scientific Publishing, Interdisciplinary Mathematical Sciences, Vol. 6, Singapore, (2007).
- [48] G. E. Fasshauer, M. J. McCourt: *Kernel-based Approximation Methods Using Matlab*, World Scientific Publishing, Interdisciplinary Mathematical Sciences, Vol. 17, Singapore, (2015).
- [49] L. Fernández, T. E. Pérez and M. A. Piñar: *On Koornwinder classical orthogonal polynomials in two variables*, J. Comput. Appl. Math., **236** (2012), 3817–3826.
- [50] G. J. Gassner, F. Lörcher, C.-D. Munz and J. S. Hesthaven: *Polymorphic nodal elements and their application in discontinuous Galerkin methods*, J. Comput. Phys., **228** (2009), 1573–1590.
- [51] J. W. Gibbs: *Fourier’s Series*, Nature, **59** (1898), 200.
- [52] R. L. Hardy: *Multiquadric equations of topography and other irregular surfaces*, J. Geophys. Res., **76** (1971), 1905–1915.
- [53] N. J. Higham: *The numerical stability of barycentric Lagrange interpolation*, IMA J. Numer. Anal., **24** (2004), 547–556.
- [54] K. Hormann, G. Klein and S. De Marchi: *Barycentric rational interpolation at quasi-equidistant nodes*, Dolomites Res. Notes Approx., **5** (2012), 1–6.
- [55] E. J. Kansa: *Application of Hardy’s multiquadric interpolation to hydrodynamics*, Proceeding Multiconference on Computer Simulation: Aerospace, San Diego (1986), 111–117.
- [56] M. Krebsbach, B. Trauzette and A. Calzona: *Optimization of Richardson extrapolation for quantum error mitigation*, preprint on ResearchGate (21 January 2022).
- [57] D. Kosloff, H. Tal-Ezer: *A modified Chebyshev pseudospectral method with an $O(N^{-1})$ time step restriction*, J. Comput. Phys., **104** (1993), 457–469.
- [58] M. Koushki, E. Jabbari and M. Ahmadiania: *Evaluating RBF methods for solving PDEs using Padua points distribution*, Alexandria Eng. J., **59** (5) (2020), 2999–3018.
- [59] O. Landon-Cardinal, L. C. G. Góvia and A. A. Clerk: *Quantitative Tomography for Continuous Variable Quantum Systems*, Phys. Rev. Lett., **120** (9) (2018), 090501.
- [60] N. T. Lloyd: *Approximation Theory and Approximation Practice*, SIAM, (2013).
- [61] G. Mastroianni, D. Occorsio: *Optimal systems of nodes for Lagrange interpolation on bounded intervals. A survey.*, J. Comput. Appl. Math., **134** (1-2) (2001), 325–341.
- [62] J. C. Merino: *Lissajous Figures and Chebyshev Polynomials*, College Math. J., **32** (2) (2003), 122–127.
- [63] C. R. Morrow, T. N. L. Patterson: *Construction of Algebraic Cubature Rules Using Polynomial Ideal Theory*, SIAM J. Numer. Anal., **15** (5) (1978), 953–976.
- [64] Numerical computing with functions: Chebfun. www.chebfun.org
- [65] R. Pachón, L. N. Trefethen: *Barycentric-Remez algorithms for best polynomial approximation in the chebfun system*, BIT Numer. Math., **49** (2009), 721–741.
- [66] D. Poggiali, D. Cecchin, C. Campi and S. De Marchi: *Oversampling errors in multimodal medical imaging are due to the Gibbs effect*, Mathematics, **9** (12) (2021), 1348.
- [67] L. Qu: *Copula density estimation by Lagrange interpolation at the Padua points*, Conference on Data Science, Statistics & Visualization 2017, Book of abstracts p. 67.
- [68] T. Rivlin: *An Introduction to the Approximation of Functions*, Dover Pub. Inc, (1969).
- [69] G. Rodeghiero, Y. Zhong et al.: *An efficient interpolation for calculation of the response of composite layered material and its implementation in MUSIC imaging*, Proceedings 19th Conference on the Computation of Electromagnetic Fields COMPUMAG, Budapest (Hungary) (2013).
- [70] L. Romani, M. Rossini and D. Schenone: *Edge detection methods based on RBF interpolation*, J. Comput. Applied Math., **349** (2019), 532–547.
- [71] C. Runge: *Über empirische Funktionen und die Interpolation zwischen äquidistanten Ordinaten*, Zeit. Math. Phys., **46** (1901), 224–243.
- [72] B. Schölkopf, A. J. Smola: *Learning with Kernels: Support Vector Machines, Regularization, Optimization, and Beyond*, MIT Press, Cambridge, MA, USA, (2002).
- [73] I. J. Schoenberg: *Metric spaces and completely monotone functions*, Ann. of Math., **39** (1938), 811–841.
- [74] L. L. Schumaker: *Spline Functions - Basic Theory*, Wiley-Interscience, New York, (1981).
- [75] A. Sommariva, M. Vianello: *Computing approximate Fekete points by QR factorizations of Vandermonde matrices*, Comp. Math. App., **57** (2009), 1324–1336.

- [76] A. Sommariva, M. Vianello and R. Zavello: *Nontensorial Clenshaw–Curtis cubature*, Numer. Algorithms, **49** (2008), 409–427.
- [77] I. H. Sloan, R. S. Womersley: *Extremal systems of points and numerical integration on the sphere*. Adv. Comput. Math., **21** (2004), 107–125.
- [78] M. A. Taylor, B. A. Wingate and R. E. Vincent: *An algorithm for computing Fekete points in the triangle*, SIAM J. Numer. Anal., **38** (5) (2000), 1707–1720.
- [79] P. Vértesi: *On the Lebesgue function and Lebesgue constant: a tribute to Paul Erdős*, Bolyai Society of Mathematical Studies, Vol. 11, Budapest, Janos Bolyai Math. Soc., (2002), 705–728.
- [80] H. Wendland: *Scattered Data Approximation*, Cambridge Monographs on Applied and Computational Mathematics, Cambridge Univ. Press, (2005).
- [81] Wikipedia: Padua points https://en.wikipedia.org/wiki/Padua_points
- [82] Y. Xu: *Christoffel functions and Fourier series for multivariate orthogonal polynomials*, J. Approx. Theory, **82** (1995), 205–239.
- [83] P. Zitnan: *The collocation solution of Poisson problems based on approximate Fekete points*, Eng. Anal. Bound. Elem., **35** (2011) 594–599.

STEFANO DE MARCHI
UNIVERSITY OF PADOVA
DEPARTMENT OF MATHEMATICS "TULLIO LEVI-CIVITA"
35122, PADOVA PD, ITALY
ORCID: 0000-0002-2832-8476
E-mail address: stefano.demarchi@unipd.it